Reducing Spurious PLL Tones in Spectrum Sensing Architectures

Shang-Kee Ting and Ali H. Sayed
Electrical Engineering Department
University of California, Los Angeles, CA 90095
Email: {tshangke,sayed}@ee.ucla.edu

***Abstract*—In a non-ideal PLL circuit, leakage of the reference signal into the control line produces spurious tones. When the distorted PLL signal is used in an analog-to-digital converter (ADC), it creates spurious tones in the sampled data as well. In spectrum sensing applications, the presence of spurious tones can lead to false detection of signals in otherwise empty channels. In a typical spectrum sensing application, there usually exists a Fourier transform block. We propose an algorithm to use this block to estimate the jitter errors from the spurious sidebands and to compensate the distorted samples in the digital domain.**

***Index Terms*—PLL, sideband suppression, spurious tones**

I. Introduction

In the design of a phase-locked loop (PLL) frequency synthesizer, an important impairment is the presence of spurious tones. The spurious tones result from leakage of the reference signal into the control line of the voltage-controlled oscillator (VCO). When the sampling clock with spurious tones is used in the ADC, spurious sidebands are introduced into the sampled data. In applications like spectrum sensing in cognitive radios, spurious tones from primary signals might give a false positive detection on actual free channels.

Conventional ways to mitigate the problem include improving the linearity of the charge pump and using large capacitors in the loop filter. Other approaches [1]–[3] include increasing the complexity of the circuit design. For example, reference [1] proposed using multiple phase frequency detectors (PFD) and charge pumps that operated in delay with respect to one another. Reference [2] proposed adding another PFD, integrators and voltage-controlled current sources. Moreover, to improve the performance of a fractional-N PLL, reference [3] used a quantizer to replace the delta-sigma modulator that is usually used and added components for charge pump offset and sampled loop filter.

These techniques are done mainly in the circuit domain. We propose a solution that relies on using digital signal processing techniques. There already exist works that handle various types of distortions in the ADC via the digital signal processing route. For example, in [4], a technique was proposed to remove jitter in narrowband signals with the help of a reference signal. This method was improved in [5] and used to handle jitter errors in OFDM signals. References [6], [7] extended the method to bandpass signals with an input reference signal. Reference [8] proposed a technique that shifts a training signal up to a suitable band to perform jitter estimation and data compensation. Reference [9] analyzed the effects of finite aperture time and sampling jitter in wideband data acquisition systems. Furthermore, reference [10] solved a problem in front-end ADC circuitry involving nonlinear frequency-dependent errors using calibration signals.

Our previous work on reducing the effects of PLL sideband distortions was described in [11]. This paper extends the work from using a sinusoidal reference signal to using a general periodic reference signal and proposes a jitter estimation method that relies on the use of a Fourier transform block (a common building block in wideband applications like spectrum sensing). The paper proposes a modification to a spectrum sensing architecture by first performing jitter estimation on a training sinusoidal signal and then switching to compensating the distorted samples to obtain the dejittered samples for spectrum sensing.

This work was supported in part by DARPA contract N66001-09-1-2029.

II. Effects of Leakage on Clock Signal

In [12], [13], a voltage-controlled oscillator (VCO) is described as a circuit that generates a periodic clock signal, $s(t)$, whose frequency is a linear function of a control voltage, V_{cont}. Let the gain of the VCO and its "free running" frequency be denoted by K_{vco} and f_s, respectively. The generated clock signal is described by

$$s(t) = A_s \sin\left(2\pi f_s t + K_{\text{vco}} \int_{-\infty}^{t} V_{\text{cont}} dt\right) \tag{1}$$

To attain some desired oscillation frequency, V_{cont} is set to some constant value. However, the generated signal, $s(t)$, may not be an accurate tone. To attain good frequency synthesis, a down-sampled version of the clock signal is fed into a block that consists of a phase-frequency detector (PFD), a charge pump (CP) and a low-pass filter (LPF) as shown in Figure 1. The PFD/CP/LPF block

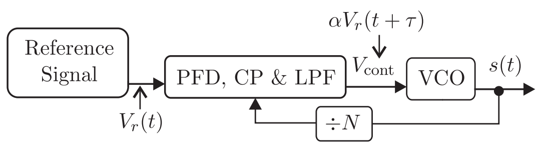

Fig. 1. Block diagram of a PLL

compares the down-converted frequency clock signal with a low-frequency reference signal at f_{ref} and makes adjustments to V_{cont}. Due to imperfections in the circuitry, the reference signal leaks into the control line of the VCO. For simplicity, we assume that the desired clock signal at f_s is obtained when V_{cont} is 0. The reference signal is assumed to be some periodic signal with fundamental frequency f_{ref} [14]. A periodic signal can be described by its Fourier series representation. For illustration purposes, we assume that the periodic signal is a triangular waveform whose Fourier series representation is

$$V_r(t) = \frac{8}{\pi^2} \sum_{k=0}^{\infty} \frac{(-1)^k}{(2k+1)^2} \sin((2k+1)2\pi f_{\text{ref}} t) \tag{2}$$

Now, suppose there is leakage and V_{cont} is

$$V_{\text{cont}} = \sum_{k=0}^{\infty} V_k \cos\left(2\pi f_k t + \theta_k\right) \tag{3}$$

where

$$\begin{aligned}\theta_k &= 2\pi f_{\text{ref}}(2k+1)\tau - \frac{\pi}{2} \\ V_k &= V_0 \frac{(-1)^k}{(2k+1)^2} \\ f_k &= (2k+1) f_{\text{ref}}\end{aligned} \tag{4}$$

for some $\{V_0, \tau\}$. Then the output of the VCO becomes

$$s(t) = A_s \sin\left(2\pi f_s t + \sum_{k=0}^{\infty} C_k \sin(2\pi f_k t + \theta_k) + \phi_s\right) \tag{5}$$

where ϕ_s is some unknown phase offset and

$$C_k = \frac{K_{\text{vco}}}{2\pi f_k} V_k \tag{6}$$

We will be analyzing the signal model with respect to an arbitrary reference time. Using a change of variables, let $t = t' - \frac{\phi_s}{2\pi f_s}$, and substitute t into equations (3) and (5). The new equations are similar to the original equations except that ϕ_s is 0. Therefore, we can let $\phi_s = 0$ without loss of generality. Applying a first order approximation to (5), some analysis gives

$$\begin{aligned} s(t) \approx A_s \sin(2\pi f_s t) + \sum_{k=0}^{\infty} \Bigg[& \frac{A_s C_k}{2} \sin(2\pi(f_s + f_k)t + \theta_k) \\ & - \frac{A_s C_k}{2} \sin(2\pi(f_s - f_k)t - \theta_k) \Bigg] \end{aligned} \tag{7}$$

This expansion shows that the distorted sampling clock signal contains multiple sidebands at $f_s \pm f_k$. Now the actual sampling instants of an ADC that uses a clock signal of the form of (5) are the zero-crossings of $s(t)$. Using (5) and defining $T_s = 1/f_s$, the sampling instants, t_n, of the ADC must satisfy the condition:

$$t_n + \sum_{k=0}^{\infty} \frac{C_k}{2\pi f_s} \sin(2\pi f_k t_n + \theta_k) = nT_s \tag{8}$$

Some analysis will show that the zero-crossings occur at times $t_n = nT_s + e(n)$, where

$$e(n) \approx -\sum_{k=0}^{\infty} \frac{C_k}{2\pi f_s} \sin(2\pi f_k n T_s + \theta_k) \tag{9}$$

We omit the derivation for brevity. Let us analyze the effect of this distorted sampling on a pure sinusoidal training tone. Let the input signal to the ADC be

$$w(t) = A_w \cos(2\pi f_w t + \phi_w) \tag{10}$$

Then the sampled signal, $\breve{w}(n)$, is approximated as

$$\begin{aligned}\breve{w}(n) &\approx w(nT_s + e(n)) \\ &\approx w(n) + e(n)\,\dot{w}(n)\end{aligned} \tag{11}$$

where $w(n) = w(t)|_{t=nT_s}$ and $\dot{w}(n) = \dot{w}(t)|_{t=nT_s}$. The term $e(n)\,\dot{w}(n)$ in (11) can be verified to be of the form

$$\begin{aligned} e(n)\dot{w}(n) = \sum_{k=0}^{\infty} \frac{f_w A_w C_k}{2 f_s} [& \cos(2\pi(f_w - f_k)nT_s + \phi_w - \theta_k) \\ & - \cos(2\pi(f_w + f_k)nT_s + \phi_w + \theta_k)] \end{aligned} \tag{12}$$

The above shows that the sampled data consists of the input signal and multiple frequency components at $f_w \pm f_k$. If the Fourier series coefficients of the reference signal in the PLL decreases rapidly, then the higher frequencies components in (9) and (12) can be ignored.

Moreover, it is possible to relate the power of the sidebands in the sampled data (12) to the sidebands in the sampling clock (7). For example, suppose the power ratio of the sideband at $f_s + f_0$ of the clock, $s(t)$, to the tone at f_s is -50dBc, then C_0 is 6.32×10^{-3}. Thus, the power of the sideband at $f_w + f_0$ of the sampled data can be derived. As an example, the reference signal is simulated as a triangular wave with a fundamental frequency of 20MHz and is approximated using the first 4 fourier series coefficients. A training signal at 45MHz is distorted by the sampling distortions and its power spectral density (PSD) is shown in fig. 2. From the plot, only the sidebands at 25MHz, 65MHz and 105MHz are detected (ie the effects from the first 2 fourier series coefficients).

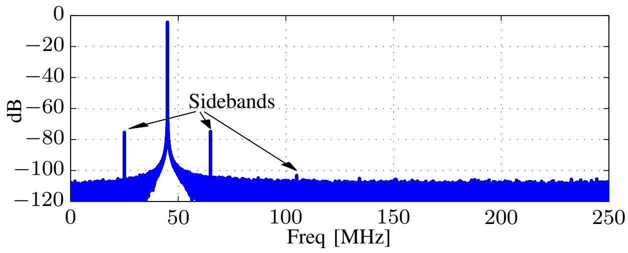

Fig. 2. The plot shows the PSD of the distorted training signal.

III. PROPOSED SOLUTION

In a typical spectrum sensing application, there is usually a module that performs Short Time Fourier Transformation (STFT) with windowing functions. To save computation and hardware complexity, we will use this module as a building block in our proposed solution. Figure 3 shows the proposed architecture. We assume that the PLL is in tracking mode (when the loop is in lock) and the distortions to the sampled data due to the PLL sidebands can be estimated from a sinusoidal training tone $w(t)$. The distorted sampled data $\breve{w}(n)$ are used with the STFT module to estimate the sampling jitters. Once the jitters (9) are estimated, the circuit switches and starts sampling the desired input signal and the sampled data is de-jittered in the digital domain before the spectrum sensing application.

A. Jitter estimation

We can use the results in (12) to evaluate the sampling offsets' parameters $\{C_k, \theta_k\}$ in (9) from the sidebands present in $\breve{w}(n)$. First, we express (10) as

$$w(n) = A_w \cos(2\pi f_w n T_s + \phi_w) \tag{13}$$

Let us assume we have estimated the amplitude and phase of the tones in (12). Let $Z(f) = Ae^{j\theta}$ denote the complex representation of the estimated amplitude A and phase θ at frequency f. Then, using (13) and (12), C_k can be estimated from the relation

$$\hat{C}_k = \frac{2f_s}{f_w}\left|\frac{Z(f_w - f_k)}{Z(f_w)}\right| = \frac{2f_s}{f_w}\left|\frac{Z(f_w + f_k)}{Z(f_w)}\right| \tag{14}$$

Let * denote complex conjugation. The phase θ_k can be estimated as

$$\begin{aligned}\hat{\theta}_k &= \arg[Z(f_w) Z^*(f_w - f_k)] \\ &= \arg\left[Z^*(f_w) Z(f_w + f_k) e^{-i\pi}\right]\end{aligned} \tag{15}$$

The question now is how to estimate the sinusoidal sidebands to enable evaluation of $\{\hat{C}_k, \hat{\theta}_k\}$ through (14) and (15). As mentioned before, in spectrum sensing applications, there is a module that performs STFT with windowing. Essentially, this module splits the data

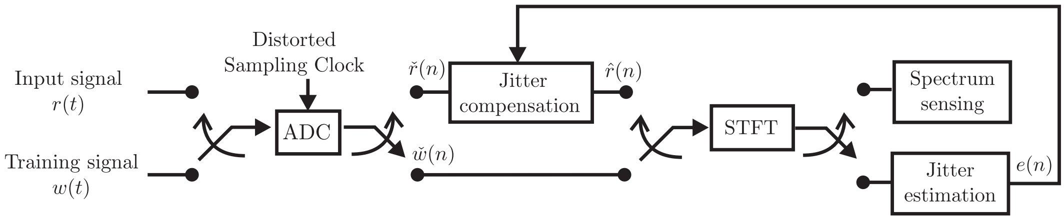

Fig. 3. Proposed architecture for reducing the effects of PLL sideband reductions in spectrum sensing applications.

into different frequency bins for further processing. The operation of the STFT is as follows [15].

In the m-th iteration of STFT, an N-point Fast Fourier Transform (N-FFT) is applied on an N-point data sequence with a windowing function $w_1(n)$. Let us assume that data sequences do not overlap and let us denote the data sequences by $x(n+Nm)$. Thus, the STFT output is

$$X(m,k) = \sum_{n=0}^{N-1} w_1(n)x(n+Nm)e^{-j2\pi\frac{k}{N}n} \tag{16}$$

where k is a particular frequency bin in the N-FFT. Suppose we want to estimate the amplitude and phase of a sinusoid at frequency f_p in a signal of the form:

$$\begin{aligned} x(n) &= \sum_{i=0}^{P} A_i \cos(2\pi f_i n T_s + \theta_i) \\ &= \sum_{i=0}^{P} \frac{A_i}{2}\left[e^{j(2\pi f_i T_s n+\theta_p)} + e^{-j(2\pi f_i T_s n+\theta_p)}\right] \end{aligned} \tag{17}$$

and only the sinusoid lies in the p-th frequency bin, then the STFT output of the bin is

$$X(m,p) = X_p(m,p) + X_n(m,p) \tag{18}$$

where

$$\begin{aligned} X_p(m,p) &= A_p\left[a_p e^{j(2\pi f_p T_s N m+\theta_p)} + b_p e^{-j(2\pi f_p T_s N m+\theta_p)}\right] \\ a_p &= \frac{1}{2}\sum_{n=0}^{N-1} w_1(n)e^{j2\pi(f_pT_s-\frac{p}{N})n} \\ b_p &= \frac{1}{2}\sum_{n=0}^{N-1} w_1(n)e^{-j2\pi(f_pT_s+\frac{p}{N})n} \end{aligned} \tag{19}$$

The $X_n(m,p)$ are nuisance terms involving the rest of the frequency components in $x(n)$ that are out of the p-th frequency band of the FFT. Using proper windowing functions $w_1(n)$, we can attenuate the effect of $X_n(m,p)$. As an example, a STFT using 1024-pt FFT is applied on the training signal shown in Fig. 2. The STFT output in the frequency bin that contains the sideband tone at 65MHz is extracted and its frequency spectrum is plotted in Fig. 4. The left and right plots show the result when no windowing is used, i.e., $w_1(n) = 1$ and when a Blackman-Harris window is used, respectively. As shown, the window function reduces the spectral leakage of out-of-band signals into the frequency channel.

Thus, manipulating $X(m,p)$ yields

$$\begin{aligned} d_p(m) &\triangleq \frac{1}{|a_p|^2-|b_p|^2}\left[\begin{array}{cc} a_p^* & -b_p \end{array}\right]\left[\begin{array}{c} X(m,p) \\ X(m,p)^* \end{array}\right] \\ &= A_p e^{j\theta_p} e^{j2\pi f_p T_s N m} + \nu(m) \\ &= Z(f_p)e^{j2\pi f_p T_s N m} + \nu(m) \end{aligned} \tag{20}$$

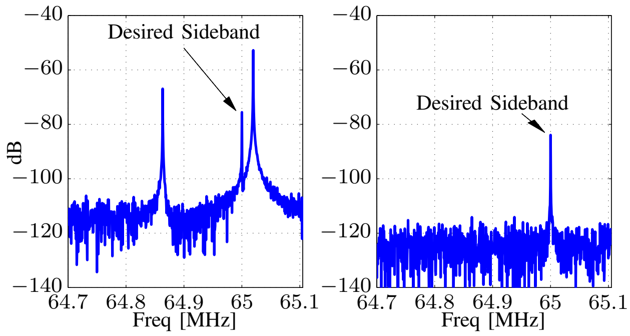

Fig. 4. The plots show the frequency domain output of a frequency channel in the STFT when no windowing is used (left) and windowing is used (right).

where $\nu(m)$ is some noise residual in terms of $X_n(m,p)$. Thus, we can estimate $Z(f_p)$ from the data $d_p(m)$ using M samples. The jitter estimation algorithm can be summarized as:

Jitter Estimation Algorithm

1) Evaluate the STFT (16) of the distorted training signal $\check{w}(n)$.
2) Use (20) on the channels that contains the training signal and its sidebands to obtain the data $d_p(m)$.
3) Use M samples of $d_p(m)$ to estimate the parameters of each sideband $Z(f_p)$.
4) Use (14) and (15) to estimate $\{\hat{C}_k, \hat{\theta}_k\}$.
5) Use (9) to estimate $e(n)$.

B. Jitter compensation

We use a similar method to our previous works [8], [11] to dejitter the sampled data. The desired data, $r(n)$, can be expressed as:

$$\begin{aligned} r(n) &\triangleq r(nT_s) \\ &= r\left(nT_s + e(n) - e(n)\right) \\ &\approx r(nT_s+e(n)) - e(n)\dot{r}(nT_s+e(n)) \\ &= \check{r}(n) - e(n)\dot{r}(nT_s+e(n)) \end{aligned} \tag{21}$$

where $\check{r}(n)$ are the distorted samples, $e(n)$ are the estimated sampling errors (see (9)), and $\dot{r}(nT_s+e(n))$ are the derivatives of $r(t)$ at $t = nT_s + e(n)$. A block diagram showing the de-jittering process is illustrated in Fig. 5. The derivatives can be approximated using a discrete filter applied to $\tilde{r}(n)$. In this current paper, a 15-tap filter is derived using a norm-1 criterion. The frequency response is shown in fig. 6.

IV. Simulations

Some simulations are done to illustrate the performance of the proposed solution. The simulation parameters are as follows. The

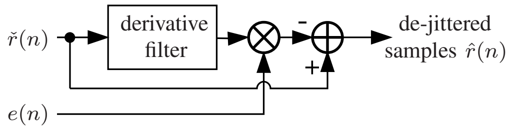

Fig. 5. Block diagram of the sideband suppression scheme.

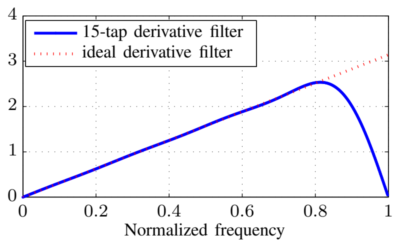

Fig. 6. The plot shows the frequency response of the derivative filter.

sampling frequency f_s is 500MHz and the reference signal in the PLL is assumed to be a triangular wave with fundamental frequency f_{ref} of 20MHz. C_0 is set to 6.32×10^{-3} so that the power ratio of the spurious sideband at $f_s \pm f_{\mathrm{ref}}$ to the signal at f_s is -50dB. The Fourier series representation of the triangular wave is truncated to the first 4 coefficients. Since the coefficients decrease rapidly, the effects of the 3rd and above coefficients are not observable in both the training signal in Fig. 2 and even when the input signal frequency is high (see Fig. 7 ahead). The frequency of the training tone, f_w, is 45MHz. We first estimate the spurious sidebands that are 20MHz and 60MHz from the distorted training signal. Then, we switch to sample the input signal and compensate the sampled data to obtain the dejittered samples. The input signal is simulated as a sinusoidal tone ranging from 25MHz to 200MHz in steps of 25MHz and the distortion suppression performance are averaged over 50 runs. The amplitude of the training signal and the input signal is set to 0.9 and white Gaussian noise with standard deviation of 1×10^{-3} is added to the input of the ADC. Finally, the STFT uses a 1024-pt FFT with a Blackman-Harris windowing function and the length of the data $d_p(m)$, M, is chosen from the set {64, 128, 256, 512, 1024}.

Figure 7 shows a realization where the desired input signal's frequency is 200MHz. The left plot shows the PSD of the signal before compensation and the right plot shows the result using the proposed method. It can be seen that the spurious sidebands are reduced by 11 to 34 dB.

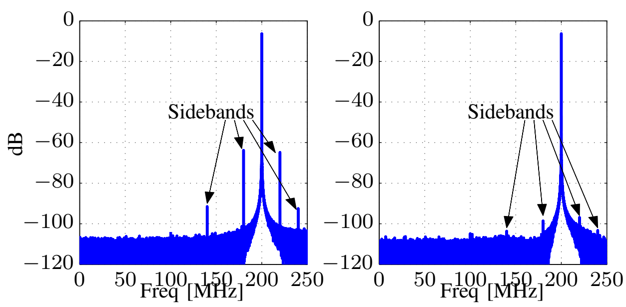

Fig. 7. The plot shows the PSD of a 200MHz input signal before and after compensation.

Figure 8 shows the sideband performance. From Fig. 7, the PLL sideband induces sidebands that are 20MHz and 60Mhz away from the input tone. The left plot in Fig. 8 shows the the reduction of the sideband power at 20MHz and 60MHz away from the input signal using M=1024 samples of $d_p(m)$. The right plot shows the average sideband performance when M is varied. The simulations show that when M=1024, the algorithm reduces the sideband distortions at 20MHz and 60MHz from the input tone by an average of 35dB and 8dB respectively.

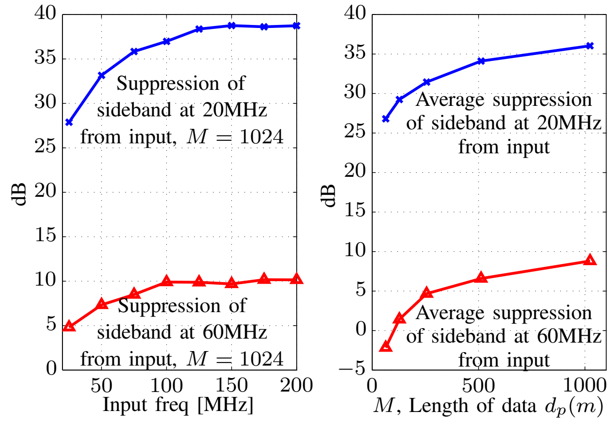

Fig. 8. The plots show the sideband suppression performance at 20MHz and 60MHz away from the input frequency signal and when M is varied.

REFERENCES

[1] T.-C. Lee and W.-L. Lee, "A spur suppression technique for phase-locked frequency synthesizers," in *Proc. ISSCC*, San Francisco, USA, Feb. 2006, pp. 2432–2441.

[2] H. Wang, G. Shou, and N. Wu, "An adaptive frequency synthesizer architecture reducing reference sidebands," in *Proc. IEEE ISCAS*, Island of Kos, Greece, 2006, pp. 3081–3084.

[3] K. J. Wang, A. Swaminathan, and I. Galton, "Spurious tone suppression techniques applied to a wide-bandwidth 2.4 GHz Fractional-N PLL," *IEEE Journal of Solid-State Circuits*, vol. 43, no. 12, pp. 2787–2797, Dec. 2008.

[4] R. Rutten, L. J. Breems, and R. H. M. van Veldhoven, "Digital jitter-cancellation for narrowband signals," in *Proc. IEEE ISCAS*, 2008, pp. 1444–1447.

[5] V. Syrjala and M. Valkama, "Jitter mitigation in high-frequency bandpass-sampling OFDM radios," in *Proc. IEEE WCNC*, Budapest, Hungary, Apr 2009, pp. 1–6.

[6] V. Syrjala and M. Valkama, "Sampling jitter estimation and mitigation in direct RF sub-sampling receiver architecture," in *Proc. IEEE ISWCS*, Siena-Tuscany, Italy, Sep 2009, pp. 323–327.

[7] V. Syrjala and M. Valkama, "Sampling jitter cancellation in direct-sampling radio," in *Proc. IEEE WCNC*, Sydney, Australia, Apr 2010, pp. 1–6.

[8] Z. J. Towfic, S.-K. Ting, and A. H. Sayed, "Sampling clock jitter estimation and compensation in ADC circuits," in *Proc. IEEE ISCAS*, Paris, France, May 2010, pp. 829–832.

[9] H Kobayashi and et al., "Finite aperture time and sampling jitter effects in wideband data acquisition systems," in *Proc. ARFTG Conf. Digest*, Anaheim, CA, USA, May 2000, vol. 38, pp. 1–7.

[10] P. Nikaeen and B. Murmann, "Digital compensation of dynamic acquisition errors at the front-end of high-performance A/D converters," *IEEE Journal of Selected Topics in Signal Processing*, vol. 3, no. 3, pp. 499–508, 2009.

[11] S.-K. Ting and A. H. Sayed, "Reduction of the effects of spurious PLL tones on A/D converters," in *Proc. IEEE ISCAS*, Paris, France, May 2010, pp. 3985–3988.

[12] G.-C. Hsieh and J. C. Hung, "Phase-locked loop techniques: A survey," *IEEE Transactions on Industrial Electronics*, vol. 43, no. 6, pp. 609–615, Dec. 1996.

[13] R.E. Best, *Phase-Locked Loops, Design, Simulation, and Applications, 5th Edition*, McGraw-Hill, 2003.

[14] F.M. Gardner, *Phaselock Techniques*, Wiley-Blackwell, 2005.

[15] A.V. Oppenheim, R.W. Schafer, and J.R. Buck, *Discrete-Time Signal Processing*, Prentice-Hall, 1999.